JOURNAL OF CHEMICAL & ENGINEERING DATA

ARTICLE

pubs.acs.org/jced

Solubility of Dibenzothiophene in Sub- and Supercritical Propane

Fabiola Martínez, Alicia Martín, and Jesusa Rincón*

Department of Chemical Engineering, Faculty of Environmental Sciences and Biochemistry, Universidad de Castilla-La Mancha, Avda. Carlos III, s/n, 45071 Toledo, Spain

ABSTRACT: The solubility of dibenzothiophene (DBT) in sub- and supercritical propane has been measured using a static view cell at pressures from (2.7 to 8.0) MPa and temperatures from (298 to 405) K. The values of the mole fraction of DBT varied from $1.3 \cdot 10^{-3}$ to $4.8 \cdot 10^{-2}$ over the experimental range studied. These values are 2 orders of magnitude higher than those reported in the literature for DBT in CO_2 at similar values of reduced pressure and temperature, which is indicative of the excellent solvent properties of propane for the extraction of polyaromatic compounds, compared to CO_2. On the other hand, when comparing the solubility of DBT in propane to that of other polyaromatic hydrocarbons (PAHs), it is found that DBT solubility (sulfur PAH) is at least 1 order of magnitude larger than that of anthracene, which in turn is 1 order of magnitude larger than that of carbazole (nitrogen PAH). These results can be mainly attributed to the effect of the vapor pressure of the solutes and, to a lesser extent, to their polarity. The experimental data have been correlated by the Peng–Robinson equation of state using two sets of mixing rules for the calculation of mixture parameters a_M and b_M, obtaining values of the average percentage deviation (APD) of 17 % and 18 %. Likewise, the empirical equation of Chrastil was used to model the experimental data, yielding a slightly higher APD (20 %).

1. INTRODUCTION

Dibenzothiophene (DBT) is a polycyclic aromatic sulfur hydrocarbon (PASH). PASHs are abundant in petroleum, coal tars, and wastewaters from petroleum and coal liquefaction industries.[1] They are toxic and/or mutagenic,[2] bioconcentrate more significantly than sulfur-free polycyclic aromatic compounds,[3] and accumulate in sediments, plants, and animal tissues.[4,5] They are also among the most refractory compounds in the residuals at contaminated sites.[4]

The low biodegradability of PASHs suggests that physical–chemical methods may be more effective than biological methods for both the remediation of PASH-contaminated soils or sediments[6] and the treatment of PASH-containing wastes.[7] Moreover, for some specific situations, such as highly polluted but relatively narrow spots (e.g., local spilled persistent organic pollutants), the supercritical fluid extraction (a physical-chemical treatment) has been shown to be a good choice to be used as remediation technology.[8−10]

Considering all this and taking into account that one of the most important properties (along with the mass transfer coefficients) that must be determined to design effective supercritical extraction processes is the solubility of the target solute in the supercritical fluid, the solubility of DBT in supercritical propane is analyzed and discussed in this work. DBT has been selected for the study as a PASH model compound because DBT and its alkylated analogues are among the most abundant PASHs in crude oils.[11] Propane has been the solvent of choice because it has been recently demonstrated that it presents better solvent properties than CO_2 for high molecular weight aromatic hydrocarbons.[12,13]

Specifically, the objectives of this study are (a) to measure the solubility of DBT in high pressure propane, at temperatures and pressures ranging from (298 to 405) K and from (2.7 to 8.0) MPa, and (b) to model the experimental data using the Peng–Robinson equation of state with two sets of mixing rules and the Chrastil equation.[14,15] To the best of our knowledge, there is no literature available on the solubilities of DBT in compressed propane.

2. EXPERIMENTAL SECTION

2.1. Materials and Experimental Setup. The solubility of DBT in propane has been measured in an experimental setup (R100CW) supplied by Thar Technology, Inc. (Pittsburgh, PA) shown in Figure 1. The setup consists of a view cell (volume 0.1 L) with two sapphire windows mounted 90° apart for the observation and recording of the phase behavior inside the cell using a camera and an illumination source. It is equipped with a pressure transducer, a temperature controller (with embedded heaters), a high pressure motor-driven mixer, and a pressure pump (P-50, Thar Technology). A cooling system was used to cool the propane before it was pumped to the solubility determination equipment. The camera, which was connected to a personal computer, allowed the observation and recording of the phase behavior inside the cell under all of the pressure and temperature conditions tested. For decompressing the system, a metering valve MV with a heating device was used. A filter protected the metering valve against potential blockage due to solidification of DBT during decompression.

Propane (mass fraction 0.995, Praxair) and DBT (mass fraction 0.980, Aldrich) were employed without further purification. The main physical properties of DBT and propane are shown in Table 1. The molar volumes of propane were obtained from the National Institute of Standards and Technology (NIST).[17]

Special Issue: Kenneth N. Marsh Festschrift

Received: February 18, 2011
Accepted: March 18, 2011
Published: March 29, 2011

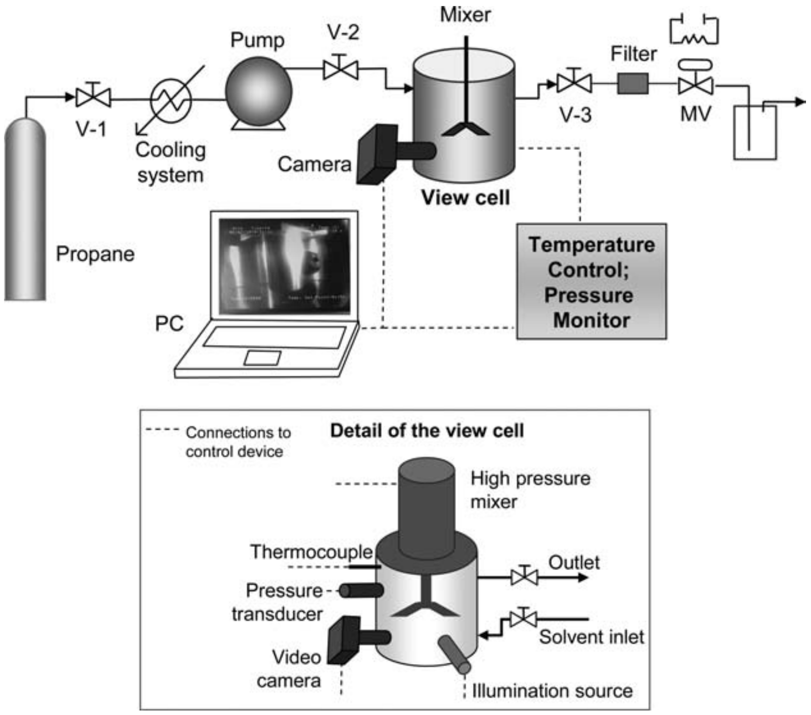

Figure 1. Layout of the experimental setup.

Table 1. Molar Mass (M), Normal Boiling Temperature (T_{bp}), Melting Temperature (T_{mp}), Critical Temperature (T_c), Critical Pressure (P_c), and Acentric Factor (ω) of DBT and Propane

	M	T_{bp}	T_{mp}	T_c	P_c	
compound	$g \cdot mol^{-1}$	K	K	K	MPa	ω
propane	44.09562[a]	231.06[b]	85.5[c]	369.825[d]	4.24733[b]	0.1518[e]
DBT	184.25692[a]	605.7[f]	371.816[g]	897[g]	3.86[g]	0.397[g]

[a] Value taken from ref 16. [b] Value taken from ref 17. [c] Value taken from ref 18. [d] Value taken from ref 19. [e] Value taken from ref 20. [f] Value taken from ref 21. [g] Value taken from ref 22.

The vapor pressure of DBT ($P^{vap}{}_{DBT}$) was calculated by eq 1, which was obtained by correlating the experimental data reported by Hansen and Eckert[23] (temperature range (303 to 348) K) and by Chirico et al.[22] (temperature range (373 to 405) K), for the experimental range of temperature studied in this work. Figure 2 shows the linear correlation ($R^2 = 0.9981$) of these data.[22,23] The average percentage deviation of vapor pressures calculated from this equation is 10.3 %.

$$\ln(P^{vap}_{DBT}/\text{Pa}) = 31.9 - \frac{10633}{T/\text{K}} \tag{1}$$

2.2. Experimental Procedure. To obtain the solubility data, a given amount of DBT was placed inside the cell. After that, the cell was closed and heated up to a given temperature by means of the embedded heaters and the temperature controller. Once the set temperature was reached, the mixer was switched on and the propane pumped into the cell. To determine the DBT solubility, the pressure was increased (at isothermal conditions) in short intervals of (0.2 to 0.4) MPa until the point at which only one phase was observed through the sapphire window. Between intervals, the pressure was held for about 5 min before the next increase. The experiments were recorded in the PC connected to the camera. This allowed the subsequent viewing of the phase equilibrium images with their corresponding real-time pressure and temperature data. The solubility was determined from the amounts of DBT and propane loaded into the cell.

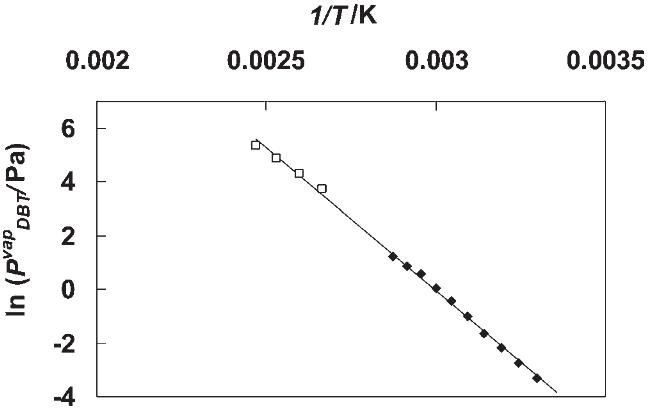

Figure 2. Vapor pressure of DBT ($P^{vap}{}_{DBT}$): ◆, values taken from ref 22; ☐, values taken from ref 23. Solid line: linear correlation of the experimental values ($\ln (P^{vap}{}_{DBT}) = -10633 \cdot (1/T) + 31.85$, where $P^{vap}{}_{DBT}$ is expressed in Pa, and T is expressed in K; $R^2 = 0.9981$).

The experimental pressure and temperature conditions used in each experiment are marked in Figure 3, where the regions for liquid, vapor, and supercritical states of propane are also indicated. Dotted lines are also drawn in Figure 3 to indicate the quasi-isobars at which the temperature effect was investigated.

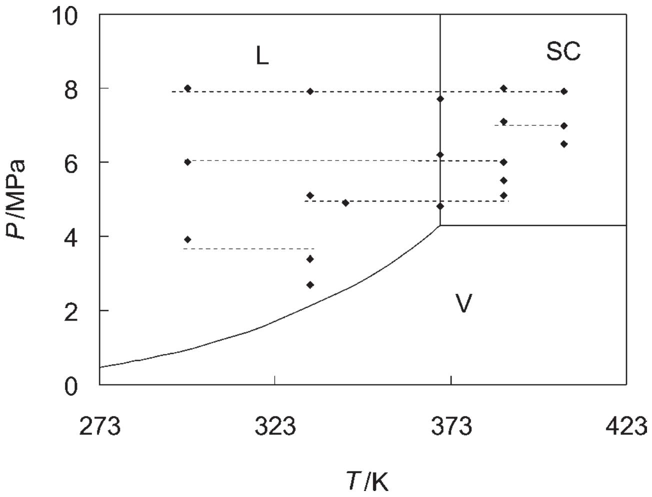

Figure 3. Experimental conditions and quasi-isobars marked in the phase diagram of propane.

Table 2. Experimental Results of Solubility of DBT in Propane

T/K	P/MPa	equilibrium phases[a]	y_2[b]	uncertainty[c] $\Delta y_2 \cdot y_2^{-1}$
298	3.9	solid—liquid	$3.20 \cdot 10^{-3}$	$2.30 \cdot 10^{-2}$
	6.0	solid—liquid	$4.75 \cdot 10^{-3}$	$2.30 \cdot 10^{-2}$
	8.0	solid—liquid	$5.51 \cdot 10^{-3}$	$2.29 \cdot 10^{-2}$
333	2.7	solid—liquid	$9.58 \cdot 10^{-3}$	$2.28 \cdot 10^{-2}$
	3.4	solid—liquid	$1.32 \cdot 10^{-2}$	$2.27 \cdot 10^{-2}$
	5.1	solid—liquid	$1.53 \cdot 10^{-2}$	$2.27 \cdot 10^{-2}$
	7.9	solid—liquid	$2.07 \cdot 10^{-2}$	$2.26 \cdot 10^{-2}$
343	4.9	solid—liquid	$1.65 \cdot 10^{-2}$	$2.27 \cdot 10^{-2}$
370	4.8	solid—supercritical	$3.42 \cdot 10^{-2}$	$2.22 \cdot 10^{-2}$
	6.2	solid—supercritical	$3.80 \cdot 10^{-2}$	$2.22 \cdot 10^{-2}$
	7.7	solid—supercritical	$4.81 \cdot 10^{-2}$	$2.19 \cdot 10^{-2}$
388	5.1	liquid—supercritical	$1.28 \cdot 10^{-3}$	$2.38 \cdot 10^{-2}$
	5.5	liquid—supercritical	$9.80 \cdot 10^{-3}$	$2.28 \cdot 10^{-2}$
	6.0	liquid—supercritical	$2.07 \cdot 10^{-2}$	$2.25 \cdot 10^{-2}$
	7.1	liquid—supercritical	$2.98 \cdot 10^{-2}$	$2.23 \cdot 10^{-2}$
	8.0	liquid—supercritical	$4.00 \cdot 10^{-2}$	$2.21 \cdot 10^{-2}$
405	6.5	liquid—supercritical	$4.04 \cdot 10^{-3}$	$2.30 \cdot 10^{-2}$
	7.0	liquid—supercritical	$1.00 \cdot 10^{-3}$	$2.28 \cdot 10^{-2}$
	7.9	liquid—supercritical	$2.03 \cdot 10^{-2}$	$2.26 \cdot 10^{-2}$

[a] Nature of the phases in equilibrium (solute—solvent). [b] Mole fraction of DBT in propane. [c] Relative combined standard uncertainty of DBT mole fraction.

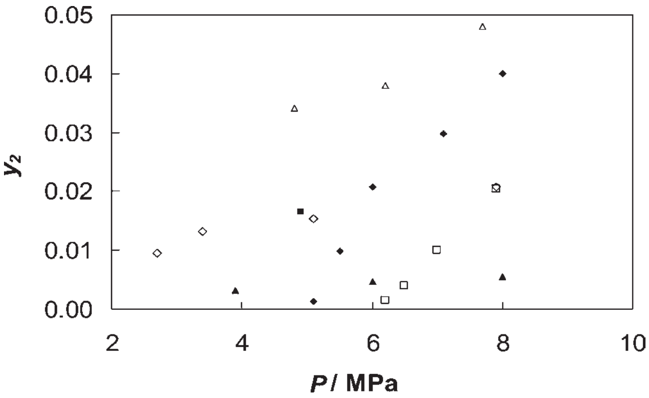

Figure 4. Experimental solubility of DBT in propane as a function of pressure and temperature: ▲, 298 K; ◇, 333 K; ■, 343 K; △, 370 K; ◆, 388 K; □, 405 K.

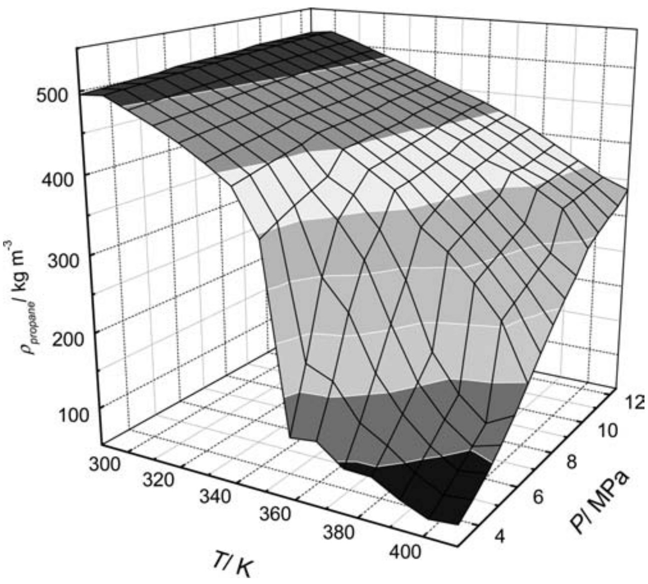

Figure 5. Variation of propane density (ρ_{propane}) with pressure and temperature in the experimental range investigated. Data obtained from NIST.[17].

Finally, it should be mentioned that according to the manufacturer's specifications of the equipment, the standard uncertainty in the cell volume was 0.08 mL, and the possible pressure and temperature variations in the cell were in the ranges ± 0.2 MPa and ± 3 °C, respectively. On the other hand, the uncertainty associated with the propane density was 2.3 %, as estimated on the basis of three major influences: pressure and temperature effects on the density and the uncertainty in the reference data for the density.[24] According to the relationship between mass and density of propane (i.e., $m_{\text{propane}} = \rho \cdot V$, in which ρ and V are the propane density and the cell volume, respectively), the relative combined standard uncertainty in the propane mass, $u_r(m_{\text{propane}})$, was 0.023 [i.e., $u_r(m_{\text{propane}}) = \Delta m_{\text{propane}}/m_{\text{propane}} = 0.023$]. The uncertainty in the mass of DBT was 0.5 mg, according to the balance calibration certificate and the manufacturer recommendations. The standard uncertainties in the DBT and propane molar masses[16] were (0.00626 and 0.00142) g·mol^{-1}, respectively. Lastly, all of these uncertainty data and an error propagation analysis[25,26] allowed the uncertainty in the DBT mole fraction to be estimated. The results obtained are shown in Table 2. It can be observed that, in all cases, the relative uncertainty in the mole fraction of DBT, $u_r(y_2)$, is less than or equal to 0.024 [i.e., $u_r(y_2) = \Delta y_2/y_2 \leq 0.024$]. This value was subsequently confirmed through repeatability tests.

3. RESULTS AND DISCUSSION

Table 2 and Figure 4 show the solubilities of DBT in propane at the experimental conditions investigated. Molar fractions of DBT varied from 0.0013 to 0.0480, what is equivalent to solubilities from (5.37 to 210.96) (mg of DBT)·(g of propane)$^{-1}$.

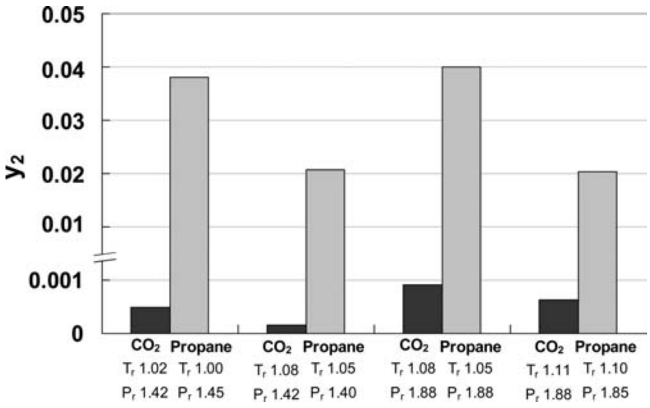

Figure 6. Comparison of DBT solubility in propane (this work) and CO_2.[29] $T_r = T/T_c$; $P_r = P/P_c$. Black bar, mole fraction of DBT in CO_2; gray bar, mole fraction of DBT in propane.

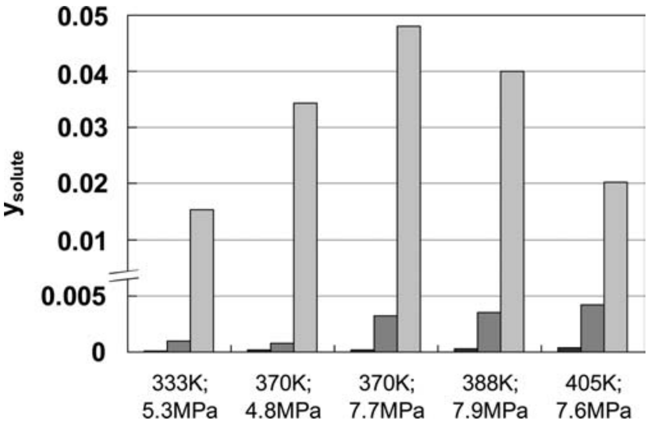

Figure 7. Solubility of carbazole, anthracene, and DBT in propane, expressed as mole fraction of solute. Black bar, carbazole; dark gray bar, anthracene; light gray bar, DBT.

It can be observed that in all cases the solubility of DBT increases by isothermically increasing the pressure, although the effect is more marked for temperature values above the critical temperature of propane (370 K). On the other hand, for a constant value of pressure, solubility values present a maximum at the critical temperature of propane; that is, solubility increases with temperature at temperatures values below 370 K, but it decreases with increasing temperature above 370 K.

These results are closely related to the influence of pressure and temperature on the density of the solvent and the solute vapor pressure, which are the main parameters affecting the solubility.[27,28] Specifically, the higher is the solvent density, the larger its solvent power and, consequently, the solute solubility; on the other hand, the higher the solute vapor pressure is the larger its solubility. Regarding the solvent density, Figure 5 shows the variation of propane density as a function of pressure and temperature in the experimental range studied.[17] This parameter increases with isothermal increases of the pressure; on the contrary, it decreases by increasing the temperature for a constant value of pressure, being this effect stronger above the critical pressure and temperature. With regard to the solute vapor pressure, it increases exponentially with the temperature.[22,23]

Bearing in mind all of this, pressure increases must lead to solubility increases of DBT in propane (because of the higher propane density). However, increases of temperature may cause contrary effects: decreases in the solvent power due to the decrease of propane density, and increases in DBT solubility due to the higher solute vapor pressure. According to the experimental results, it can be inferred that for temperature values below the critical temperature, the effect of the solute vapor pressure on DBT solubility dominates over that of solvent density, so temperature increases lead to higher solubilities. On the other hand, for temperate values over 370 K, the abrupt decrease of propane density by increasing the temperature produces the decrease of the solute solubility, the effect of solvent density being stronger than that of the solute vapor pressure.

3.1. Comparison of the Solubility of DBT in Propane and in Carbon Dioxide. As carbon dioxide is the supercritical solvent most commonly used, the results for the solubility of DBT in propane have been compared to those of DBT in carbon dioxide previously reported.[29] Figure 6 shows the mole fraction of DBT in both solvents for similar values of the reduced pressure (P_r) and temperature (T_r). The treatment of data in this manner avoids the influence of the proximity to the solvent's critical point (propane: T_c, 369.8 K, P_c, 4.25 MPa; carbon dioxide: T_c, 304.1 K, P_c, 7.38 MPa). It can be observed that, in all of the experimental conditions studied, the solubility of DBT in propane is 2 orders of magnitude higher than in carbon dioxide. This behavior has been also observed in previous works of our group for different PAH compounds (concretely anthracene and carbazole)[12,13] and highlights the superior solvent properties of propane for hydrocarbons against carbon dioxide.[30−32]

3.2. Comparison of the Solubility of DBT, Anthracene, and Carbazole in Propane. The solubility of DBT (sulfur PAH) in propane has been compared to that of anthracene (PAH) and carbazole (nitrogen PAH), obtained in previous works of our group.[12,13] The values of solubility (expressed as mole fraction of solute) of these three PAH compounds in propane are summarized in Figure 7, for similar operation conditions (T, P). Specifically, the temperature values used for the comparison were the same in all cases, while the pressure values differed less than 0.5 MPa (the pressures shown in Figure 7 are the average of the three pressure conditions compared).

Carbazole presents the lower values of solubility at the experimental conditions studied, being the maximum mole fraction obtained $4.2 \cdot 10^{-4}$. In the case of anthracene, it is $4.2 \cdot 10^{-3}$, that is, 1 order of magnitude higher than that of carbazole. Nevertheless, the solubility of DBT is in all cases at least 1 order of magnitude larger than that of anthracene.

These differences must be attributed to the vapor pressure of the solutes and the interactions between the different solutes with the solvent (propane), which are influenced by their polarity. Table 3 shows the values of the vapor pressure of the three PAH solutes for the different temperatures studied, together with their ground-state dipole moments (μ_g).

With regard to the interaction between the solvent and the solutes, it must be considered that propane is a nonpolar solvent (molecular dipole moment near 0, $\mu_g = 0.084$ D)[41] and therefore, its affinity for nonpolar solutes its higher than for polar ones. Thus, according to the polarity (molecular dipole moment) the solute solubility in propane should follow the order antracene ($\mu_g = 0.0$ D) > DBT ($\mu_g = 0.8$ D) > carbazole ($\mu_g = 1.8$ D). On the other hand, as said before, the higher is the solute vapor pressure, the larger its solubility. Therefore, on the basis of the solute vapor pressure, the PAH solute solubility should follow the order DBT ≫ anthracene > carbazole.

Table 3. Molar Mass (M), Structure, Ground State Dipole Moment (μ_g), and Vapor Pressure ($P^{vap}{}_{solute}$) of the Polyaromatic Solutes Compared

Solute	M/g·mol^{-1}	Structure	μ_g/ D	$P^{vap}{}_{solute}$ [d]/ MPa			
				333 K	370 K	388 K	405 K
Carbazole	167.20660	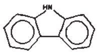	1.8±0.1[a]	$1.442 \cdot 10^{-08}$	$5.585 \cdot 10^{-07}$	$2.571 \cdot 10^{-06}$	$9.599 \cdot 10^{-06}$
Anthracene	178.22920		0.0[b]	$7.822 \cdot 10^{-08}$	$2.384 \cdot 10^{-06}$	$9.927 \cdot 10^{-06}$	$3.399 \cdot 10^{-05}$
Dibenzothiophene	184.25692	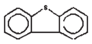	0.8[c]	$9.587 \cdot 10^{-07}$	$2.695 \cdot 10^{-05}$	$1.079 \cdot 10^{-04}$	$3.570 \cdot 10^{-04}$

[a] Value taken from ref 33 and 34. [b] Value taken from ref 35 and 36. [c] Value taken from ref 37 and 38. [d] Value taken from ref 39 for carbazole, 40 for anthracene, and 22 and 23 for DBT.

In view of the experimental results, it may be stated that in the experimental systems investigated the effect of the solute vapor pressure on the solute solubility dominates over that of the polarity, especially in the case of the solubility values reported for DBT and anthracene (higher solubility of DBT). Both parameters influencing the solute solubility (solute vapor pressure and polarity) explain that carbazole is the least soluble PAH of the three solutes compared in this work.

3.3. Modeling of the Solubility of DBT in Propane with Peng–Robinson Equation of State and with Chrastil Equation. The experimental values of the solubility obtained have been correlated in order to find mathematical expressions that allow the prediction of the solubility of DBT in propane at different operation conditions.

The Peng–Robinson equation of state (eq 2) can be used to predict the phase behavior of multicomponent systems.[14] Parameters $a(T)$ and b are defined by eqs 3 and 4.

$$P = \frac{R \cdot T}{v - b} - \frac{a(T)}{v \cdot (v + b) + b \cdot (v - b)} \tag{2}$$

$$a_i(T) = 0.45724 \cdot \frac{R^2 \cdot T_{C,i}{}^2}{P_{C,i}} \cdot \left(1 + (0.37464 + 1.54226 \cdot \omega_i - 0.26992 \cdot \omega_i{}^2) \cdot \left(1 - \sqrt{\frac{T}{T_{C,i}}}\right)\right)^2 \tag{3}$$

$$b_i = 0.07780 \cdot \frac{R \cdot T_{C,i}}{P_{C,i}} \tag{4}$$

For multicomponent systems, mixture parameters a_M and b_M are estimated by the expressions given in eq 5. In these equations a_{ij} and b_{ij} represent the interaction parameters for whose calculation different sets of mixing rules are reported in the literature.[12,14,42,43]

$$a_M = \sum_i \sum_j y_i \cdot y_j \cdot a_{ij} \text{ and } b_M = \sum_i \sum_j y_i \cdot y_j \cdot b_{ij} \tag{5}$$

The set of mixing rules used by Peng and Robinson[14] to estimate interaction parameters (a_{ij} and b_{ij}) was the *one-fluid van der Waals set of rules*, which is defined by eq 6 (where $k_{ij} = k_{ji}$, $k_{ii} = 0$). This set of mixing rules, labeled S1 in this work, implies the use of only one adjustable parameter (k_{ij}).

$$\mathbf{S1}: a_{ij} = \sqrt{a_i \cdot a_j} \cdot (1 - k_{ij}) \text{ and } b_{ij} = (b_1 + b_2)/2 \tag{6}$$

Likewise, a set of mixing rules involving two adjustable parameters (k_{ij} and δ_{ij}) has been used. It is labeled S2 and defined by eq 7 (where $k_{ij} = k_{ji}$, $k_{ii} = 0$, $\delta_{ij} = \delta_{ji}$, $\delta_{ii} = 0$). This set has been used by our group in previous works yielding good correlation of the experimental results.[12,13]

$$\mathbf{S2}: a_{ij} = \sqrt{a_i \cdot a_j} \cdot (1 - k_{ij}) \text{ and } b_{ij} = \sqrt{b_i \cdot b_j} \cdot (1 - \delta_{ij}) \tag{7}$$

To find the optimal values of the adjustable parameters, the Newton method has been used to minimize the average percentage deviation (APD), the objective function given by eq 8 that compares the experimental (y_2) and calculated ($y_2{}^{cal}$) solubility (expressed as mole fraction of DBT).

$$\text{APD} = \left(\sum_{i=1}^{n} \frac{|y_{2,i} - y_{2,i}^{cal}|}{y_{2,i}} \right) \cdot \frac{(100\%)}{n} \tag{8}$$

The optimal values of the adjustable parameters of the Peng–Robinson equation with mixing rules sets S1 and S2, together with the APD values, are shown in Table 4. It can be seen that the set of mixing rules S2 presents a slightly smaller value of the APD (~17 %) and therefore the best adjustment results, which can be attributed to the fact that it involves the use of two adjustable parameters instead of one adjustable parameter used by S1. Likewise, to give a visual idea of the correlation, Figure 8 shows the estimated data versus the experimental ones for both sets of mixing rules tested (S1 and S2). It can be observed a good fitting of the experimental results in all cases.

On the other hand, the Chrastil equation has been also evaluated for the correlation of the experimental data obtained in this work. The Chrastil model relates the solubility of a solute (y_2) in a fluid at high pressure with the density of the fluid (ρ) and the temperature (T), as shown in eq 9.[15] Despite the simplicity of this equation, it is often used as it provides good correlation of the experimental data:

$$\ln y_2 = a_0 + \frac{a_1}{T} + a_2 \cdot \ln \rho \tag{9}$$

where a_0, a_1, and a_2 are adjustable parameters. In this work, they have been calculated by minimizing the objective function given by eq 8, which compares the experimental (y_2) and the calculated ($y_2{}^{cal}$) values of the mole fraction of DBT. Table 4 shows the values of the optimal adjustable parameters and the APD obtained by the correlation of experimental data with the Chrastil equation (~ 20 %).

It can be observed that the APD is slightly higher than that obtained by using the Peng–Robinson equation of state, despite

Table 4. Optimal Values of the Adjustable Parameters of the Peng−Robinson Equation (Using Set of Mixing Rules S1 and S2) and Chrastil Equation. Absolute Percentage Deviation (APD) between the Calculated and the Experimental Solubility Values for the Different Equations Evaluated

equation	mixing rules set	parameter					APD/%
		k_{12}	δ_{12}	a_0	a_1	a_2	
Peng−Robinson	S1	0.0380	-	-	-	-	18.50
	S2	0.0825	−0.0791	-	-	-	17.29
Chrastil	-	-	-	−14.828	−5100.0	4.275	20.15

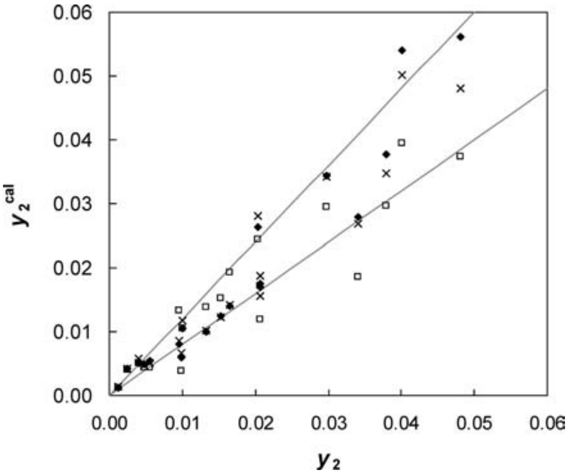

Figure 8. Comparison of the experimental solubility data with those estimated by the Peng−Robinson equation (using mixing rules sets S1 and S2) and Chrastil equation. Estimated data versus the experimental ones: ×, Peng−Robinson equation using S1; ♦, Peng−Robinson equation using S2; □, Chrastil equation. Area delimited by the two solid lines includes values of calculated mole fraction (y_2^c) with the percentage deviation below ± 20 %.

the fact that Chrastil model requires the use of three adjustable parameters, against the one or two adjustable parameters (using S1 and S2 mixing rules sets, respectively) involved in the correlation with Peng−Robinson equation. This fact can be explained taking into account that the Peng−Robinson equation is more complex and involves the use of a number of physical properties of the system components, that is not required by the equation of Chrastil because of its simplicity. Finally, the graphical comparison of the experimental and Chrastil equation predicted data is given in Figure 8. It can be observed a good agreement between experimental and estimated data.

CONCLUSIONS

The solubility of DBT in compressed propane has been measured using a static method at pressures from (2.7 to 8.0) MPa and temperatures from (298 to 405) K. The values of mole fraction of DBT in propane under the experimental conditions investigated varied from $1.3 \cdot 10^{-3}$ to $4.8 \cdot 10^{-2}$. These mole fractions are 2 orders of magnitude higher than those reported in the literature for DBT in compressed CO_2, at similar conditions of reduced temperature and pressure, and highlight the excellent solvent properties of propane for the extraction of polyaromatics, compared to CO_2. The solubility data obtained have been modeled by the Peng−Robinson equation of state, using two sets of mixing rules (that imply the use of one or two adjustable parameters) for the calculation of mixture parameters (a_M and b_M). Both sets of mixing rules yielded similar APDs, concretely, 17.3 and 18.5 %. Likewise, the empirical Chrastil equation (which involves the use of three adjustable parameters) was used to correlate the experimental solubility, giving a slightly higher APD (20.1 %). Both expressions evaluated (Peng−Robinson and Chrastil) yield a good fitting of the experimental results, so they can be used to predict the solubility with more or less accuracy (and simplicity), depending on the requirements.

AUTHOR INFORMATION

Corresponding Author

*Tel.: +34 902204100. Fax: +34 925268840. E-mail address: jesusa.rincon@uclm.es.

Funding Sources

The authors gratefully acknowledge MMAM, MCyT of Spain, and Junta de Comunidades de CLM for the financial support to this work through projects 096/2006/3-11.3, A141/2007/2-11.3, CMT 2006-10105, and PAI08-0195-3614.

REFERENCES

(1) Smith, J. H.; Mabey, W. R.; Bohonos, N.; Holt, B. R.; Lee, S. S.; Chou, T. W.; Bomberger, D. C.; Mill, T. *Environmental Pathways of Selected Chemicals in Freshwater Systems, Part II*, Report No. EPA-600/7-78-074; Environmental Protection Agency: Athens, GA, 1978.

(2) Eastmond, D. A.; Booth, G. M.; Lee, M. L. Toxicity, Accumulation, and Elimination of Polycyclic Aromatic Sulfur Heterocycles in Daphnic-Magna. *Arch. Environ. Contam. Toxicol.* **1984**, *13*, 105–111.

(3) Vassilaros, D. L.; Stoker, P. W.; Booth, G. M.; Lee, M. L. Capillary Gas-Chromatograpic Determination of Polycyclic Aromatic-Compound in Vertebrate Fish Tissue. *Anal. Chem.* **1982**, *54*, 106–112.

(4) Boehm, P. D.; Barak, J. E.; Fiest, D. L.; Elskus, A. A. A Chemical Investigation of the Transport and Fate of Petroleum-Hydrocarbons in Littoral and Benthic Environments: The TSESIS oil-spill. *Mar. Environ. Res.* **1982**, *6*, 157–188.

(5) Ogata, M.; Fujisawa, K. Organic Sulfur-Compounds and Polycyclic-Hydrocarbons Transferred to Oyster and Mussel from Petroleum Suspension-Identification by Gas-Chromatography and Capillary Mass Chromatography. *Water Res.* **1985**, *19*, 107–118.

(6) Ramírez-Verduzco, L. F.; Rojas-Aguilar, A.; de los Reyes, J. A.; Muñoz-Arroyo, J. A.; Murrieta-Guevara, F. Solid-Liquid Equilibria of Dibenzothiophene and Dibenzothiophene Sulfone in Organic Solvents. *J. Chem. Eng. Data* **2007**, *52*, 2212–2219.

(7) Akgerman, A.; Roop, R. K.; Hess, R. K.; Yeo, S.-D. Supercritical Extraction in Environmental Control. In *Supercritical Fluid Technology. Reviews in Modern Theory and Applications*; Bruno, T. J., Ely, J. F., Eds.; CRC Press: Boca Raton, FL, 1991; pp 479−509.

(8) Tavlarides, L. L.; Zhou, W.; Anitescu, G. In *Supercritical Fluid Technology for Remediation of PCB/PAH-Contaminated Soils/Sediments*, Proceedings of the 2000 Conference on Hazardous Waste Research, Denver, Colorado, USA, May 23−25, 2000; pp 239−255.

(9) Anitescu, G.; Tavlarides, L. L. Solubilities of Solids in Supercritical Fluids: II. Polycyclic Aromatic Hydrocarbons (PAHs) + CO_2/Cosolvent. *J. Supercrit. Fluids* **1997**, *11*, 37–51.

(10) Anitescu, G.; Tavlarides, L. L. Supercritical Extraction of Contaminants from Soils and Sediments. *J. Supercrit. Fluids* **2006**, *38*, 167–180.

(11) Kim, I.-K.; Jung, O.-J. Sonochemical Reaction Mechanism of a Polycyclic Aromatic Sulfur Hydrocarbon in Aqueous Phase. *Bull. Korean Chem. Soc.* **2002**, *23*, 990–994.

(12) Martínez, F.; Martín, A.; Asencio, I.; Rincón, J. Solubility of Anthracene in Sub and Supercritical Propane. *J. Chem. Eng. Data* **2010**, *55*, 1232–1236.

(13) Martínez, F.; Martín, A.; Camarillo, R.; Rincón, J. Measurement and Modelling of the Solubility of 9*H*-Carbazole in Sub- and Supercritical Propane. *J. Chem. Eng. Data*, DOI: 10.1021/je100923d.

(14) Peng, D. Y.; Robinson, D. B. A New Two-Constant Equation of State. *Ind. Eng. Chem. Fundam.* **1976**, *15*, 59–64.

(15) Chrastil, J. Solubility of Solids and Liquids in Supercritical Gases. *J. Phys. Chem.* **1982**, *86*, 3016–3021.

(16) Coplen, T. B.; Böhlke, J. K.; De Bièvre, P.; Ding, T.; Holden, N. E.; Hopple, J. A.; Krouse, H. R.; Lamberty, A.; Peiser, H. S.; Revesz, K.; Rieder, S. E.; Rosman, K. J. R.; Roth, E.; Taylor, P. D. P.; Vocke, R. D.; Xiao, Y. K. Isotope-Abundance Variations of Selected Elements (IUPAC 476 Technical Report). *Pure Appl. Chem.* **2002**, *74*, 1987–2017.

(17) Lemmon, E. W.; McLinden, M. O.; Friend, D. G. Thermophysical Properties of Fluid Systems. *NIST Chemistry WebBook, NIST Standard Reference Database Number 69*; Linstrom, P. J., Mallard, W. G., Eds.; National Institute of Standards and Technology: Gaithersburg, MD, 2005; http://webbook.nist.gov.

(18) Streng, A. G. Miscibility and Compatibility of Some Liquid and Solidified Gases at Low Temperature. *J. Chem. Eng. Data* **1971**, *16* 357–359.

(19) Majer, V.; Svoboda, V. *Enthalpies of Vaporization of Organic Compounds: A Critical Review and Data Compilation*; Blackwell Scientific Publications: Oxford, England, 1985.

(20) Yaws, C. L. *Chemical Properties Handbook*; McGraw Hill: New York, 1999.

(21) Weast, R. C.; Grasselli, J. G. *CRC Handbook of Data on Organic Compounds*, 2nd ed.; CRC Press, Inc.: Boca Raton, FL, 1989.

(22) Chirico, R. D.; Knipmeyer, S. E.; Nguyen, A.; Steele, W. V. The thermodynamic properties of dibenzothiophene. *J. Chem. Thermodyn.* **1991**, *23*, 431–450.

(23) Hansen, P. C.; Eckert, C. A. An Improved Transpiration Method for the Measurement of Very Low Vapor Pressures. *J. Chem. Eng. Data* **1986**, *31*, 1–3.

(24) Miyamoto, H.; Watanabe, K. A Thermodynamic Property Model for Fluid-Phase Propane. *Int. J. Thermophys.* **2000**, *21*, 1045–1072.

(25) *Quantifying Uncertainty in Analytical Measurement*, 2nd ed.; Ellison, S. L. R., Rosslein, M., Williams, A., Eds.; EURACHEM/CITAC Guide 4: Prague, 2000.

(26) Taylor, B. N.; Kuyatt, C. E. *Guidelines for Evaluating and Expressing the Uncertainty of NIST Measurement Results*; NIST Technical Note 1297; National Institute of Standards and Technology: Gaithersburg, MD, 1994.

(27) Stahl, E.; Quirin, K. W.; Gerard, D. *Dense Gases for Extraction and Refining*; Springer-Verlag: Berlin, 1988.

(28) Clifford, T. *Fundamentals of Supercritical Fluids*; Oxford University Press Inc.: New York, 1999.

(29) Mitra, S.; Chen, J. W.; Viswanath, D. S. Solubility and Partial Molar Volumes of Heavy Aromatic Hydrocarbons in Supercritical CO_2. *J. Chem. Eng. Data* **1988**, *33*, 35–37.

(30) Rincón, J.; Cañizares, P.; García, M. T.; Gracia, I. Regeneration of Used Lubricant Oil by Propane Extraction. *Ind. Eng. Chem. Res.* **2003**, *42*, 4867–4873.

(31) Rincón, J.; Cañizares, P.; García, M. T. Improvement of the Waste-Oil Vacuum-Distillation Recycling by Continuous Extraction with Dense Propane. *Ind. Eng. Chem. Res.* **2007**, *46*, 266–272.

(32) Rincón, J.; Camarillo, R.; Martínez, F.; Rodriguez, L.; Ancillo, V. Correlating the Solubilities of Used Frying Oil in High-Pressure Propane, Carbon Dioxide, and Ethane. *Ind. Eng. Chem. Res.* **2011**, *50*, 1028–1033.

(33) Liptay, W. *Excited States*, Vol. 1; Lim, E. C., Ed.; Academic Press: New York, 1974; p 200.

(34) Boesiger, J.; Leutwyler, S. Van der Waals Vibrations and Binding Energies of Carbazole·Kr. *Chem. Phys. Lett.* **1986**, *126*, 238–244.

(35) Dorohoi, D. O. Electric Dipole Moments of the Spectrally Active Molecules Estimated from the Solvent Influence on the Electronic Spectra. *J. Mol. Struct.* **2006**, *792—793*, 86–92.

(36) *Hyperchem5.02*, Molecular visualization and Simulation Program Package; Hypercube, Inc.: Gainesville, FL, 1997.

(37) Charles, R. G.; Freiser, H. Electric Moments and Structure of Substituted Thiophenes. III. Polysubstituted Thiophenes. *J. Am. Chem. Soc.* **1950**, *72*, 2233–2235.

(38) Soscún, H.; Alvarado, Y.; Hernández, J.; Hernández, P.; Atencio, R.; Hinchliffe, A. Experimental and Theoretical Determination of the Dipole Polarizability of Dibenzothiophene. *J. Phys. Org. Chem.* **2001**, *14*, 709–715.

(39) Jimenez, P.; Roux, M. V.; Turrión, C. Thermochemical Properties of N-Heterocyclic Compounds III. Enthalpies of Combustion, Vapour Pressures and Enthalpies of Sublimation, and Enthalpies of Formation of 9H-Carbazole, 9-Methylcarbazole, and 9-Ethylcarbazole *J. Chem. Thermodyn.* **1990**, *22*, 121–726.

(40) Bender, R.; Bielling, V.; Maurer, G. The Vapour Pressures of Solids: Anthracene, Hydroquinone, and Resorcinol. *J. Chem. Thermodyn.* **1963**, *15*, 585–594.

(41) Lide, D. R.; Frederikse, H. P. R. *CRC Handbook of Chemistry and Physics*, 89th ed.; CRC Press: Boca Raton, FL, 2008.

(42) Shibata, S. K.; Sandler, S. I. Critical Evaluation of Equation of State Mixing Rules for the Prediction of High-pressure Phase Equilibria. *Ind. Eng. Chem. Res.* **1989**, *28*, 1893–1898.

(43) Goodarznia, I.; Esmaeilzadeh, F. Solubility of an Anthracene, Phenanthrene, and Carbazole Mixture in Supercritical Carbon Dioxide. *J. Chem. Eng. Data* **2002**, *47*, 333–338.